European Congress on Computational Methods
in Applied Sciences and Engineering (ECCOMAS 2012)
J. Eberhardsteiner et.al. (eds.)
Vienna, Austria, September 10-14, 2012

WEAR PREDICTION IN THE RAILWAY FIELD: DEVELOPMENT OF A MODEL FOR THE STUDY OF THE WHEEL AND RAIL PROFILE EVOLUTION

M. Ignesti[1], **L. Marini**[1], **E. Meli**[1] **and A. Rindi**[1]

[1]Department of Energy Engineering, University of Florence, Italy
Via S. Marta n. 3, 50139 Firenze, Italy
e-mail: ignesti@mapp1.de.unifi.it, marini@mapp1.de.unifi.it
e-mail: meli@mapp1.de.unifi.it, rindi @mapp1.de.unifi.it

Keywords: wheel-rail wear, wheel-rail contact, multibody modeling of railway vehicles

Abstract. *The prediction of wheel and rail wear is a fundamental issue in the railway field, both in terms of vehicle stability and in terms of economic costs (planning of maintenance interventions). In this work the Authors present a wear model specifically developed for the evaluation of the wheel and rail profile evolution, the layout of which is made up of two mutually interactive but separate units: a vehicle model for the dynamical analysis and a model for the wear evaluation. The first one consists of two parts that interact online during the dynamic simulations: a 3D multibody model of the railway vehicle and an innovative 3D global contact model for the detection of the contact points between wheel and rail and for the calculation of the forces in the contact patches. The wear model starts from the outputs of the dynamic simulations (position of contact points, contact forces and global creepages) and calculates the pressures inside the contact patches through a local contact model; then the material removed due to wear is evaluated (by means of experimental laws correlating the friction power produced by the tangential contact forces and removed material by wear) and the worn profiles of wheel and rail are obtained.*

Subsequently the new model has been compared with the wear evaluation procedure implemented in Simpack, a widely tested and validated multibody software for the analysis of the railway vehicle dynamics; the comparison aims both to evaluate the model performance (in terms of accuracy and efficency) and to further validate the wear model (just tested, as regards the weel wear prediction, in previous works related to the critical Aosta-Pre Saint Didier line). The Simpack wear procedure layout is similar to that of the developed model: the main difference is the absence of the local contact model inside the wear model because of the global wear approach used by this software.

The comparison has been carried out considering a benchmark train composed by a locomotive (E.464) and a passengers vehicle (Vivalto) provided by Trenitalia while the simulations have been performed on a mean Italian railway line (obtained by means of a statistical analysis based on the data relative to the whole Italian railway net provided by Rete Ferroviaria Italiana).

1 INTRODUCTION

In this work the Authors will present an innovative model to estimate the evolution of the wheel and rail profiles due to wear based on a combination of multibody and wear modeling; subsequently an exhaustive comparison with the wear evaluation model implemented in the Simpack commercial multibody software is performed both in terms of accuracy and efficency performance and to further validate the wear model (in addition to the wheel wear analysis carried out in previous works [4]). In more details the general model layout is made up of two mutually interactive parts: the *vehicle model* (multibody model and 3D global contact model) and the *wear model* (local contact model, wear evaluation and profiles update). The multibody model of the vehicle is implemented in Simpack environment and accurately reproduces the vehicle dynamics taking into account all the significant degrees of freedom. The 3D global contact model, developed by the Authors in previous works [3], detects the wheel-rail contact points by means of an innovative algorithm based on suitable semi-analytic procedures and then, for each contact point, calculates the contact forces through Hertz's and Kalker's theory [6]. As regards the wear estimation, the procedure is based on a local contact model (in this case the Kalker's FASTSIM algorithm) and on a wear model exploiting an experimental relationship for the calculation of the removed material. The wear model, starting from the outputs of the local contact model (pressures and local creepages), calculates the total amount of removed material due to wear and its distribution along the wheel and rail profiles. The removal of the material is carried out considering the different time scales characterizing the wear evolution on the wheel and on the rail. The wear model implemented in Simpack software [1] uses a global approach to the wear estimation that does not consider any local model for the contact patch investigation with a model precision loss. With the only exception of the local contact model, the general architecture is similar to that of the new wear model; in this way an accurate comparison between the models has been possible in terms of accuracy and efficency.

The train set to be investigated in order to evaluate the capability in wear estimation of the two compared wear models is a train composition widely used in Italian railways made up of a locomotive (E.464) and a passenger vehicle (Vivalto) the technical data of which have been provided by Trenitalia. All the simulations are performed on a virtual track, specifically designed to represent a statistical description of the whole Italian railway net [4]. The data necessary to build the virtual track model have been provided by RFI.

2 GENERAL ARCHITECTURE OF THE MODEL

In this section the layout of the two considered wear models will be described; the innovative model developed in this work is indicated as UNIFI model, while the benchmark model implemented within the Simpack multibody software is marked with SIMPACK model [1].

The UNIFI model, developed in collaboration with Trenitalia and RFI, is made up of two main parts: the vehicle model and the wear model (see Fig. 1).

The vehicle model aims to simulate the vehicle dynamics and is composed by the multibody model of the railway vehicle that in this work consists of a locomotive (E.464) and of a passengers vehicle (Vivalto) (a vehicle configuration widely used in the Italian railway net) and by the 3D global contact model; the two subsystems interact online during the dynamic simulations at each time integration step creating a loop. In more detail the first one evaluates the kinematic variables (positions, orientations and their derivates) of the wheelset and consequently of each wheel-rail contact pair while the second one, starting from these quantities, calculates the global contact variables (position of the contact points, geometry of the contact patches by means of

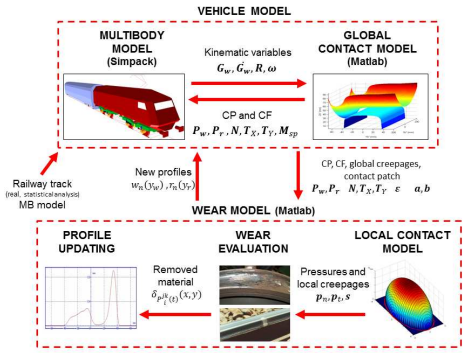

Figure 1: General Architecture of the UNIFI Model.

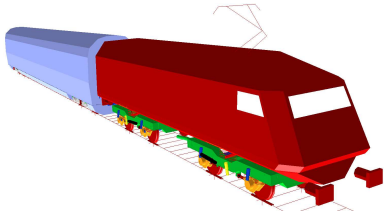

Figure 2: Global view of the multibody model.

the evaluation of its semiaxes, contact forces and global creepages) that are then passed to the multibody model in order to continue the simulation of the vehicle dynamics. The 3D global contact model carries out both the detection of the contact points thanks to an innovative algorithm developed by the authors in previous works [3] and the evaluation of the contact forces using Hertz's and Kalker's global theories [6]; the algorithm does not introduce any simplifying hypothesis on the geometry and kinematics of the contact problem and can be implemented directly online without using look-up table for the evaluation of the contact variables. The dynamic simulations has been performed with the Simpack multibody commercial software: the multibody model has been built directly in Simpack environment while the global contact model, implemented in C/C++ environment, has been customized by means of the Simpack *User Routine module* (implemented in FORTRAN environment) capable of handle the interaction between Simpack and routines defined by users. The railway track is the other main input of the vehicle model; in this research activity the mean Italian railway line has been considered, approached by means of a statistical analysis starting from the data relative to the whole Italian railway net (provided by RFI) and consisting of an ensemble of N_c curvilinear tracks, each of length equal to l_{track}, characterized by a radius value R, a sopraelevation h, a suitable velocity V and a statistical weight factor p_k; this approach is obviously necessary because of the length and the complexity of the considered track that would make both its multibody modeling and the computational load impractical. The outputs of the vehicle model represent also the input of the wear model and are the global contact variables evaluated during all the N_c dynamic simulations.

The wear model has been fully implemented in Matlab environment and is made up of three distinct phases: the local contact model, the wear evaluation and the profile update. Starting from the global contact variables, the local contact model (based both on the Hertz's local theory and on the simplified Kalker's algorithm FASTSIM) evaluates the local contact parameters (the contact pressures and the local creepages) and divides the contact patches into adhesion and slip zone. Then, within the slip area, the distribution of removed material both on the wheel and on the rail surface is calculated by means of an experimental law that correlates the volume of removed material with the frictional dissipated energy at the contact interface. Finally the profiles of wheel and rail are updated removing the material from the original profiles. The new profiles are the outputs of one discrete step of the whole model loop and have to be passed back to the vehicle model in order to proceed with the wear cycle calculating the vehicle dynamics with the updated profiles.

The evolution of the wheel and rail profiles is therefore a discrete process. In this research the choice of the discrete step is a main issue and, as will be clarified in the following, has

to consider the difference between the time scales of the wheel and rail wear evolution rate. For the wheel wear prediction the total mileage km_{tot} traveled by the benchmark vehicle has to be subdivided in discrete steps with a suitable strategy and within each step (corresponding to km_{step} traveled by the vehicle) the wheel profile will be supposed to be constant. For the rail, instead, the depth of the wear does not depend on the traveled distance but on the total tonnage burden on the track and thus on the number of vehicles moving on the track; particularly the total vehicle number N_{tot} will be subdivided in discrete steps (corresponding to N_{step} vehicle on the track) within which the rail profile is supposed to be constant.

As regard the discretization strategy, the number of discrete steps should be chosen according to a good balance between the model precision and the computational load. Furthermore several types of update procedures exist [8]: the constant step and the adaptive step are the main ones. In the first one a constant update step is defined while the second one is based on the definition of a threshold value that imposes the maximum material quantity to remove at each profiles update; consequently the update step is variable. In this work the second method has been chosen because the adaptive step is more suitable to follow the nonlinear behavior of the wear evolution; in fact the wear evolution both of wheel and rail in the first phase is characterized by an higher rate (due to the initial non conformal contact between the unworn profiles) while in a second phase a slower rate due to the higher conformal contact is present.

In order to make the comparison between the two wear models more accurate, the SIMPACK model layout is similar to the UNIFI one, with the exception of the local contact model. Therefore the whole model consists of the following parts: the vehicle model fully implemented in Simpack environment (composed by the multibody vehicle and the global contact model) and the global wear model (made up of the wear evaluation direcly implemented in Simpack and the profile update realized in Matlab environment). The main difference between the two considered wear models is the approach to the wear problem: the SIMPACK model uses a global approach to the wear evaluation without taking into account the local contact variables (pressures and creepages) within the contact patch and consequently its subdivision in sliding and adhesion zone but using only the global contact variables. This aspect leads to a reduction of the computational load due to the absence of the contact patch discretization and investigation but it mainly causes a decrease of the whole model precision.

Related to the vehicle model, the multibody model is always the vehicle composition made of the locomotive (E.464) and the passengers vehicle (Vivalto) and there are no differences with respect to the UNIFI model. On the contrary, concerning the global contact model, the version implemented in the Simpack commercial software has been used. Also this model is capable of calculating the global contact forces and of detecting the multiple contact points at the wheel-rail interface; however, for the research of multiple contact points, the wheel and rail surfaces are divided in three different zones within which a single point can be detected, introducing a limitation on the number of contact points and especially on their position. In addition to the simplifying hypothesis on the geometry and kinematics of the contact problem, the Simpack contact model uses look-up table to evaluate the contact parameters with a consequently loss of the model precision. The profile update strategy has been implemented in Matlab environment in order both to reproduce the same strategy adopted in the UNIFI model and to customize the wear evaluation model implemented in Simpack (based on a different wear law with respect to the UNIFI model).

3 THE VEHICLE MODEL

In this section a brief description of the vehicle models (made up of the multibody model and the global contact model) will be given. In particular the global contact models used in the two architectures will be analyzed (the strengths and weaknesses will be emphasized); while, concerning the multibody model, the common benchmark vehicle will be presented.

3.1 The Multibody Model

A railway vehicle composition widely used in the Italian railway net comprising a E.464 locomotive and a Vivalto passenger transport unit is considered in this work (see Fig. 2).

The TRAXX 160 DCP, well known with the E.464 commercial name, is a set of light electric locomotives widely used with the passengers vehicle on short and medium distance; its physical and geometrical characteristics can be found in literature [5]. The E.464 bogies are two motor-axes ones (wheel formula B_0B_0) with two suspension stages for the rigid bodies connections (see Fig. 3).

The primary suspension stage (see Fig. 3) is composed by a rigid rod that connects the axlebox with the bogie frame by means of appropriate flexible joints, two coil springs and a damper the arrangement of which is not perfectly vertical to allow the damping of later motions between axlebox and bogie frame. The secondary suspensions connect the bogie frames to the coach and it comprises four coil springs, six dampers (the verticals ones, the laterals ones and the anti-yaw ones) and a traction rod for the bogie connection to the coach.The main characteristics of the suspensions can be found in literature [5].

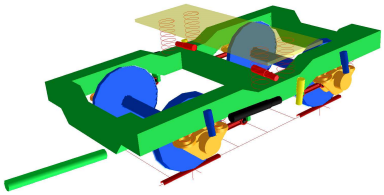

Figure 3: E.464: bogie and suspension stages.

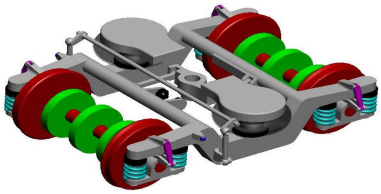

Figure 4: Vivalto: bogie and suspension stages.

The main feature of the Vivalto coach is the possibility of holding the passengers on two different levels realized in the middle of the carriage. The weight increase resulting from this configuration has led to install three ventilated brake discs for each wheelset, in order to obtain good braking performance. The main physical and geometrical properties used for the multibody model can be found in literature [5]. The Vivalto bogies are two trailer bogies with two suspension stages designed by Siemens company, marked SF-400 (see Fig. 4). The primary suspensions are composed by two coil springs and two pivots concentric with the coil springs and forced and welded on the bogie to connect the wheelset; on the pivots suitable rubber springs are fitted. With the particular realized assembly, the coil springs work only in vertical direction while the traction, brake and lateral forces act on the rubber springs. Moreover the primary suspension is equipped with two vertical bumstops (one for each coil spring) and a damper the arrangement of which is not perfectly vertical for the same reasons treated above. The secondary suspension is made up of two air springs set up in series at two ”emergency springs” which have the purpose to ensure the safety in deflated spring condition; in the modeling a single spring with the characteristic given by the springs mounted in series has been considered. In addition the suspension comprises a common zeta link for the connection between the bogie and the coach, a roll bar necessary because of the rise of the coach center of gravity due to the

two passenger levels, two lateral damper and two lateral bumpstops. The main characteristics of the suspensions can be found in literature [5].

3.2 The Global Contact Model

Dynamic simulations of railway vehicles need a reliable and efficient method to evaluate the contact points between wheel and rail, because their position has a considerable influence both on the direction and on the magnitude of the contact forces. In this section the two different global contact models used in this research will be described.

3.2.1 UNIFI Global Contact Model

The UNIFI global contact model is divided in two parts: in the first one the contact points are detected by means of an innovative algorithm developed by the Authors in previous works [3], while in the second one the global contact forces acting at the wheel-rail interface are evaluated by means of Hertz's and Kalker's global theories [6].

The algorithm for the contact points detection starts from the standard idea that the contact points make stationary the distance between the wheel and rail surfaces (see Figure 5(a)); in more details the distance has a point of relative minimum if there is no penetration between the considered surfaces, while it has a relative maximum in the other case. The innovative adopted algorithm is a fully 3D model that takes into account all the six relative degrees of freedom (DOF) between wheel and rail and it is able to support generic railway tracks and generic wheel and rail profiles; moreover it assures both a general and accurate treatment of the multiple contact without introducing simplifying assumptions on the problem geometry and kinematics (with no limits on the number of contact points detected) and highly numerical efficiency making possible the online implementation within the commercial multibody software without look-up table (in this way also the numerical performance of the commercial multibody software are improved).

Two specific reference systems have to be introduced in order to simplify both the model's equations and the definition of the wheel and rail geometrical surfaces. The auxiliary reference system and the local reference system. The auxiliary system $O_r x_r y_r z_r$ is defined on the plane of the rails and follows the motion of the wheelset during the dynamic simulations: the x_r axis is tangent to the center line of the track in the origin O_r, the position of which is defined so that the $y_r z_r$ plane contains the center of mass $\mathbf{G_w}$ of the wheelset, and the z_r axis is perpendicular to plane of the rails. The local system $O_w x_w y_w z_w$ is rigidly connected to the wheelset except for the rotation around its axis and the x_w axis is parallel to the $x_r y_r$ plane (see Figure 5(b)). In the following, for the sake of simplicity, the variables referred to the local system will be marked with the apex w, while those referred to the auxiliary system with the apex r; the variables belonging to the wheel and to the rail will be indicated with the subscripts w and r respectively.

The distance method algorithm (see Figure 5(a)) is based on a classical formulation of the contact problem in multibody field:

$$\mathbf{n}_r^r(\mathbf{P}_r^r) \wedge \mathbf{n}_w^r(\mathbf{P}_w^r) = \mathbf{n}_r^r(\mathbf{P}_r^r) \wedge R_w^r \mathbf{n}_w^w(\mathbf{P}_w^w) = \mathbf{0} \tag{1a}$$

$$\mathbf{n}_r^r(\mathbf{P}_r^r) \wedge \mathbf{d}^r = \mathbf{0} \tag{1b}$$

where $\mathbf{P}_w^w$ and $\mathbf{P}_r^r$ are the positions of the generic point on the wheel surface and on the rail surface expressed in their reference systems ($\mathbf{P}_w^w(x_w, y_w) = \begin{pmatrix} x_w & y_w & -\sqrt{w(y_w)^2 - x_w^2} \end{pmatrix}^T$ and $\mathbf{P}_r^r(x_r, y_r) = \begin{pmatrix} x_r & y_r & r(y_r) \end{pmatrix}^T$ with $w(y_w)$ and $r(y_r)$ the wheel and rail profile generating functions), $\mathbf{n}_w^w$ and $\mathbf{n}_r^r$ are

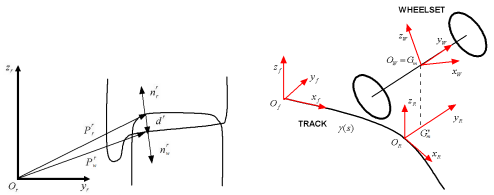

(a) (b)

Figure 5: Distance method.

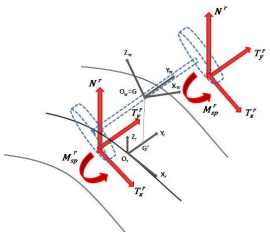

Figure 6: Contact global forces.

the outgoing normal unit vectors to the wheel and rail surface respectively, R_w^r is the rotation matrix that links the local reference system to the auxiliary one (with elements r_{ij}) and $\mathbf{d}^r$ is the distance vector between two generic points on the wheel surface and on the rail surface (both referred to the auxiliary system): $\mathbf{d}^r(x_w,y_w,x_r,y_r) = \mathbf{P}_w^r(x_w,y_w) - \mathbf{P}_r^r(x_r,y_r)$ with $\mathbf{P}_w^r = \mathbf{O}_w^r + R_w^r \mathbf{P}_w^w(x_w,y_w)$ the position of the generic point of the wheel surface expressed in the auxiliary system.

The first condition (equation (1a)) of the system (1) imposes the parallelism between the normal unit vectors, while the second one (equation (1b)) requires the parallelism between the normal unit vector to the rail surface and the distance vector. The system (1) consists of six nonlinear equations in the unknowns (x_w,y_w,x_r,y_r) (only four equations are independent and therefore the problem is 4D). However it is possible to express three of the four variables (in this case (x_w,x_r,y_r)) as a function of y_w, reducing the original 4D problem to a simple 1D scalar equation. The reduction of the problem dimension using appropriate analytical procedures is the most innovative aspect of the proposed method; from the second component of (1a) the expression $x_{w1,2}(y_w)$ can be obtained (two possible values are present); then, similarly, from the first component of (1a) the expression for $y_{r1,2}(y_w)$ can be determined and from the second component of (1b) the relation $x_{r1,2}(y_w)$. Finally, replacing the variables $x_{w1,2}(y_w)$, $x_{r1,2}(y_w)$ and $y_{r1,2}(y_w)$ in the first component of (1b), two simple scalar equations in the y_w variable have been found:

$$F_{1,2}(y_w) = -r'\left(G_{wz} + r_{32}y_w - r_{33}\sqrt{w^2 - {x_{w1,2}}^2} - b\right) - \left(G_{wy} + r_{21}x_{w1,2} + r_{22}y_w - r_{23}\sqrt{w^2 - {x_{w1,2}}^2} - y_{r1,2}\right) = 0. \tag{2}$$

The expression (2) consists of two scalar equations in the variable y_w that can be easily solved with appropriate numerical algorithms. The advantages of this approach based on the reduction of the algebraic problem dimension are many: an high numerical efficiency that makes possible the online implementation of the new method within the multibody vehicle models without look-up table is obtained, the analytical approach assures an high degree of accuracy and generality and finally the 1D problem assures an easier management of the multiple solutions from an algebraic and a numerical point of view. Thus, once obtained the generic solution (indicated with the subscript i) y_{wi} of equation (2), the complete solution (x_{wi}, y_{wi}, x_{ri}, y_{ri}) of the system (1) and consequently the contact points $\mathbf{P}_{wi}^r = \mathbf{P}_w^r(x_{wi},y_{wi})$ and $\mathbf{P}_{ri}^r = \mathbf{P}_r^r(x_{ri},y_{ri})$ can be found by substitution. Eventually the physical conditions of no penetration between wheel and rail and the convexity condition have to be satisfied so that the contact is physically possible.

Then, for each contact point the global creepages ε acting in the contact patch and the normal N^r and tangential $\mathbf{T}^r$ contact forces, evaluated by means of the Hertz's and the Kalker's global theory respectively, are determined (see Figure 6) [6].

3.2.2 SIMPACK Global Contact Model

The Simpack wear model employs the global contact model implemented in the Simpack multibody software both for the contact point evaluation and the global forces calculation [1].

The standard ORE S1002 wheel profile and UIC 60 rail profile have been introduced in Simpack by means of cubics spline approximation; however a limitation on the number of sampling profile points equal to 600 points is imposed by the software for computational time requirements unlike the UNIFI global contact model where no limitations are present. Among all the of contact point detection algorithms provided by software, the more general and suitable version has been chosen in order to compare the different models. This algorithm ensures multiple contact point detection but, at the same time, introduces a set of simplifying hypothesis:

1. a maximum of three contact points for each wheel-rail pair can be detected;

2. the wheel profile is divided in three zones noted with *tread*, *flange* and *flange2* areas: for each of these a single contact point can be found. Moreover the *flange2* corresponding to the back of the flange and thus only two actual contact points for each wheel-rail pair can be detected. This limitation on the contact points position is an important approximation on the kinematics of the contact problem;

3. suitable look-up tables for the calculation of the *tread* contact point location and of the relative tangential forces are used to have reasonable calculation times;

4. the *flange* and *flange2* contacts are calculated online without pre-calculated tables: moreover for these points the wheel-rail contact is considered rigid. With this method, discontinuities in the contact point position and other contact parameters (i.e. tangential forces) can arise when moving the wheelset laterally over the track. On the contrary the *tread* point is detected considering a quasi-elastic contact. In this case wheel and rail are regarded as qualitatively elastic by means of a special weighting and regularization function (calculated with the look-up table mentioned above): it leads to a virtual contact patch instead of a single contact points and thus no discontinuities can appear with this method. The two different approaches simultaneously used for the contact points detection could result in solver and accuracy problems.

Concerning to the global normal forces calculation the contact between wheel and rail is ensured by introducing a one-sided spring-damper element (producing a force only when there is penetration between wheel and rail surface) which moves along the profiles depending on the contact point position; the normal contact force is calculated from the equivalent penetration by means of the Hertz theory. The tangential forces evaluation, instead, both for the online calculation in the *flange* and *flange2* zones and for the look-up table calculation in the *tread* zone is based on the linear saturated Kalker theory.

4 THE WEAR MODEL

In this section the wear models will be described in details: particularly both the two different wear evaluation procedures and the common profile updating strategy will be presented. The update strategy (developed by the Authors) is necessary also for the SIMPACK model because it is not structured to make a whole wear loop and specifically it is not capable to pass back the new worn profiles to the *vehicle model*. Related to the local contact model, not present in the SIMPACK model, the Kalker FASTSIM algorithm widely used in railway applications has been utilized and its wide and exhaustive description can be found in literature [6].

4.1 The Local Contact Model

The purpose of the local contact model is the calculation of the local contact variables (normal and tangential contact stresses p_n, $\mathbf{p}_t$ and local creep $\mathbf{s}$, all evaluated within the contact patch) starting from the corresponding global variables (contact points $\mathbf{P}^r_w$, $\mathbf{P}^r_r$, contact forces N^r, T^r_x, T^r_y, global creepage ε and semiaxes of the contact patch a,b). The model is based on the Kalker's local theory in the simplified version implemented in the algorithm FASTSIM [6] and consequently on the proportionality hypothesis between the tangential contact pressure $\mathbf{p}_t$ and the elastic displacements $\mathbf{u}$, both evaluated within the contact patch: $\mathbf{u}(x,y) = L\mathbf{p}_t(x,y)$, $L = L(\varepsilon,a,b,G,\nu)$ where the flexibility L is a function of the global creepages ε, the semiaxes of the contact patch a,b, the wheel and rail combined shear modulus G and the wheel and rail combined Poisson's ratio ν [6]. The local creepages $\mathbf{s}$ can be calculated by derivation considering both the elastic creepages and the rigid ones: $\mathbf{s}(x,y) = \dot{\mathbf{u}}(x,y) + V \begin{pmatrix} \varepsilon_x \\ \varepsilon_y \end{pmatrix}$ where $V = \left\| \dot{\mathbf{O}}^r_w \right\|$ is the longitudinal vehicle speed. At this point it is necessary to discretize the elliptical contact patch in a grid of points in which the quantities p_n, $\mathbf{p}_t$ and $\mathbf{s}$ will be evaluated. Once the contact patch is discretized, the FASTSIM algorithm allows the iterative evaluation of both the contact pressures value p_n, $\mathbf{p}_t$ and the local creepage $\mathbf{s}$ in order to divide the contact patch in adhesion and slip zone. Indicating the generic point of the grid with (x_I, y_J), the normal contact pressure is calculated by means of the Hertz local theory, while for the tangential variables the following relationships hold:

$$\text{if } \|\mathbf{p}_A(x_I,y_J)\| \leq \mu p_n(x_I,y_J) \Rightarrow \begin{cases} \mathbf{p}_t(x_I,y_J) = \mathbf{p}_A(x_I,y_J) \\ \mathbf{s}(x_I,y_J) = \mathbf{0} \end{cases} \tag{3a}$$

$$\text{if } \|\mathbf{p}_A(x_I,y_J)\| > \mu p_n(x_I,y_J) \Rightarrow \begin{cases} \mathbf{p}_t(x_I,y_J) = \mu p_n(x_I,y_J)\mathbf{p}_A(x_I,y_J)/\|\mathbf{p}_A(x_I,y_J)\| \\ \mathbf{s}(x_I,y_J) = \frac{LV}{\Delta x(y_J)}\left(\mathbf{p}_t(x_I,y_J) - \mathbf{p}_A(x_I,y_J)\right) \end{cases} \tag{3b}$$

where μ is the static friction coefficient; equations (3a) and (3b) hold respectively in the adhesion and slip zone. Iterating the procedure for all the grid discretization points ($2 \leq I \leq n_x$ and successively for $1 \leq J \leq n_y$) and assuming as boundary conditions $\mathbf{p}_t(x_1,y_J) = \mathbf{0}$, $\mathbf{s}(x_1,y_J) = \mathbf{0}$ for $1 \leq J \leq n_y$ (i.e. stresses and creepages zero out of the contact patch), the desired distribution of $p_n(x_I,y_J)$, $\mathbf{p}_t(x_I,y_J)$ and $\mathbf{s}(x_I,y_J)$ can be determined.

4.2 The UNIFI Wear Evaluation

The UNIFI model uses an experimental relationship between the volume of removed material and the frictional work to evaluate the distribution of removed material on wheel and rail due to wear (assuming dry contact conditions). The relationship is able to directly evaluate the specific volumes of removed material $\delta_{P^{jk}_{wi}(t)}(x,y)$ and $\delta_{P^{jk}_{ri}(t)}(x,y)$ related to the i-th contact points $P^{jk}_{wi}(t)$ and $P^{jk}_{ri}(t)$ on the j-th wheel and rail pair during the k-th of the N_c dynamic simulations.

The calculation of $\delta_{P^{jk}_{i}(t)}(x,y)$ requires first of all the evaluation of the frictional power developed by the tangential contact stresses; to this purpose the *wear index* $I_W = \mathbf{p}_t \bullet \mathbf{s}/V$ (expressed in N/mm^2) is defined. This index, by means of appropriate experimental tests, can be correlated with the *wear rate* K_W (expressed in $\mu g/(m \cdot mm^2)$) which represents the mass of removed material for unit of distance traveled by the vehicle (expressed in m) and for unit of surface (expressed in mm^2). The experimental relation between K_W and I_W adopted is the following [4]:

$$K_W(I_W) = \begin{cases} 5.3 * I_W & I_W < 10.4 \\ 55.12 & 10.4 \leq I_W \leq 77.2 \\ 61.9 * I_W - 4723.56 & I_W > 77.2. \end{cases} \tag{4}$$

Once the wear rate $K_W(I_W)$ is known (the same both for the wheel and for the rail), the specific volume of removed material on the wheel and on the rail (for unit of distance traveled by

the vehicle and for unit of surface) can be calculated as follows (expressed in $mm^3/(m \cdot mm^2)$):

$$\delta_{P_{wi}^{jk}(t)}(x,y) = K_W(I_W)\frac{1}{\rho}, \qquad \delta_{P_{ri}^{jk}(t)}(x,y) = K_W(I_W)\frac{1}{\rho} \tag{5}$$

where ρ is the material density (expressed in kg/m^3).

4.3 The SIMPACK Wear Evaluation

The SIMPACK wear model is an add-on module of Simpack multibody software and allows the calculation of wear effects on the wheel and the rail profiles of a railway vehicle [1]. The wear evaluation is a post-processing calculation after a time domain simulation. The global wear approach leads to the estimation of the removed material starting from the global contact creapages without considering the local ones within the contact patch and therefore this quantity represents an averaged volume to be removed on all the contach patch surface, causing a possible wear overestimation.

This model is based on the wear law proposed by Krause and Poll [7] that correlates the volume of removed material for unit of distance travelled by the vehicle(K^{SIM} expressed in m^3/m) to the specific frictional power I^{SIM} dissipated in the contact patch of area A ($I^{SIM} = P_g/A$ expressed in W/mm^2: the global power is $P_g = \mathbf{T}^r \bullet \mathbf{s_g}$ where the global creapages $\mathbf{s_g} = V \begin{pmatrix} \varepsilon_x \\ \varepsilon_y \end{pmatrix}$ are expressed in m/s) by means of a proportionality law. It distinguishes between two wear regimes, *mild wear* and *severe wear*, characterized by different material removed rates: the wear coefficients, i.e. the proportionality factors between frictional work and removed material, supposed the same for wheel and rail, are available in literature [7]:

$$\begin{array}{lll} \textit{mild wear}: & C_{mild} = 9.8710 * 10^{-14}\, m^3/J & I^{SIM} < 4W/mm^2 \\ \textit{severe wear}: & C_{severe} = 9.8710 * 10^{-13}\, m^3/J = 10 * C_{mild} & I^{SIM} \geq 4W/mm^2. \end{array} \tag{6}$$

The removed material volume (for unit of length travelled by vehicle) for each rail and wheel is then calculated: $K^{SIM} = CP_g/(2 \cdot V)$ where C is the proportionality factor of equation (6) and V is the velocity of the vehicle. Finally the average removed material volume (expressed in $m^3/(m \cdot mm^2)$) in the normal direction to the profiles for the i-th contact patch of the j-th wheel and rail pair during the k-th of the N_c dynamical simulations are obtained:

$$\delta^{tot}_{P_{wi}^{jk}(t)}{}^{SIM}(y_w) = \begin{cases} 0 & y_w \leq -b_{wi}^{jk}/2 \\ \frac{K^{SIM}}{2\pi w(y_{wi}^{cjk}) \cdot b_{wi}^{jk}} & -b_{wi}^{jk}/2 \leq y_w \leq b_{wi}^{jk}/2 \\ 0 & y_w \geq b_{wi}^{jk}/2 \end{cases}, \qquad \delta^{tot}_{P_{ri}^{jk}(t)}{}^{SIM}(y_r) = \begin{cases} 0 & y_r \leq -b_{ri}^{jk}/2 \\ \frac{K^{SIM}}{l_k \cdot b_{ri}^{jk}} & -b_{ri}^{jk}/2 \leq y_w \leq b_{ri}^{jk}/2 \\ 0 & y_r \geq b_{ri}^{jk}/2 \end{cases} \tag{7}$$

where $w(y_{wi}^{cjk})$ is the wheel radius evaluated in y_{wi}^{cjk} (the trasversal position of the generic wheel contact point), l_k is the length of the k-th simulated track and b_{wi}^{jk}, b_{ri}^{jk} the generic contact patch widths. The $1/\left[2\pi w(y_{wi}^{cjk}) \cdot b_{wi}^{jk}\right]$ and $1/\left(l_k \cdot b_{ri}^{jk}\right)$ factors average the removed volume for each contact point P_i^{cjk} over the whole longitudinal development of the wheel and of the rail.

The global wear evaluation approach without local contact model for the investigation of the local variables (pressures and creepages) within the contact patch and therefore without distinction between sliding and adhesion zone in the contact area, leads to the evaluation of the mean wear volumes $\delta^{tot}_{P_{wi}^{jk}(t)}{}^{SIM}(y_w)$ and $\delta^{tot}_{P_{ri}^{jk}(t)}{}^{SIM}(y_r)$ to substract from the rail and the wheel profile uniformly along all the contact patch width b. This approximation avoids the contact patch discretization leading to a time calculation saving but obviously it cause also a decrease of the whole wear model accuracy. The outputs of the SIMPACK wear evaluation are thus the distributions of the removed material $\delta^{tot}_{P_{wi}^{jk}(t)}{}^{SIM}(y_w)$ and $\delta^{tot}_{P_{ri}^{jk}(t)}{}^{SIM}(y_r)$.

4.4 Profile Update Strategy

The profile update strategy is the set of numerical procedures that allows the calculation of the new profiles of wheel $w_n(y_w)$ and rail $r_n(y_r)$ (the profiles at the next step), starting from the old profiles of wheel $w_o(y_w)$ and rail $r_o(y_r)$ (i.e. the profiles at the current step) and all the distributions of removed material $\delta_{P_{wi}^{jk}(t)}(x,y)$, $\delta_{P_{ri}^{jk}(t)}(x,y)$ and $\delta_{P_{wi}^{jk}(t)}^{tot\ \ SIM}(y_w)$, $\delta_{P_{ri}^{jk}(t)}^{tot\ \ SIM}(y_r)$. The update strategy is necessary also to remove the numerical noise that affects the previous distributions and that can cause problems to the global contact models due to non physical alterations of the new profiles.

Except for the first step, used only in the UNIFI case, the other update procedure steps hold for the both investigated models; for the sake of semplicity the apex SIM will be omitted when the procedure steps remain the same (all the cases 2-7 except the fifth step).

1. *Longitudinal integration*:

$$\frac{1}{2\pi w(y_{wi}^{cjk})}\int_{-a(y)}^{+a(y)}\delta_{P_{wi}^{jk}(t)}(x,y)dx=\delta_{P_{wi}^{jk}(t)}^{tot}(y),\qquad \frac{1}{l_k}\int_{-a(y)}^{+a(y)}\delta_{P_{ri}^{jk}(t)}(x,y)dx=\delta_{P_{ri}^{jk}(t)}^{tot}(y) \tag{8}$$

where $w(y_{wi}^{cjk})$ is the wheel radius evaluated in y_{wi}^{jk} and l_k is the length of the k-th simulated track. This first integration is related only to the UNIFI model and sums, in the longitudinal direction, all the wear contributes inside the contact patch, averaging this quantity over the whole longitudinal development of the wheel and of the rail (by means of the factors $1/\left[2\pi w(y_{wi}^{jk})\right]$ and $1/l_k$); in other words it provides the mean value of removed material (expressed in $mm^3/(m\cdot mm^2)$). The difference between the terms $1/l_k$ and $1/\left[2\pi w(y_{wi}^{cjk})\right]$ (the track length is much greater than the wheel circumference length) is the main cause that leads the wheel to wear much faster than the rail and consequently to a different scale of magnitude of the two investigated phenomena. This reflects the physical phenomena that the life of the rail is much greater than that of the wheel.

2. *Track integration*:

$$\int_{T_{in}}^{T_{end}}\delta_{P_{wi}^{jk}(t)}^{tot}(y)V(t)dt\approx\int_{T_{in}}^{T_{end}}\delta_{P_{wi}^{jk}(t)}^{tot}(s_w-s_{wi}^{cjk}(t))V(t)dt=\Delta_{P_{wi}^{jk}}(s_w),\qquad \int_{T_{in}}^{T_{end}}\delta_{P_{ri}^{jk}(t)}^{tot}(y)V(t)dt\approx\int_{T_{in}}^{T_{end}}\delta_{P_{ri}^{jk}(t)}^{tot}(s_r-s_{ri}^{cjk}(t))V(t)dt=\Delta_{P_{ri}^{jk}}(s_r); \tag{9}$$

the track integration sums all the wear contributes coming from the dynamic simulation to obtain the depth of removed material for wheel $\Delta_{P_{wi}^{jk}}(s_w)$ and rail $\Delta_{P_{ri}^{jk}}(s_r)$ expressed in $mm = mm^3/mm^2$. In order to have a better accuracy in the calculation of the worn profiles, the natural abscissas s_w and s_r of the curves $w(y_w)$ and $r(y_r)$ have been introduced. In particular the relations $y\approx s_w-s_{wi}^{cjk}(t)$, $w(y_w)=w(y_w(s_w))=\tilde{w}(s_w)$ and $y\approx s_r-s_{ri}^{cjk}(t)$, $r(y_r)=r(y_r(s_r))=\tilde{r}(s_r)$ locally hold (see Figure 7), where the natural abscissas of the i-th contact points s_{wi}^{cjk} and s_{wi}^{cjk} can be evaluated from their positions P_{wi}^{jk} and P_{ri}^{jk}.

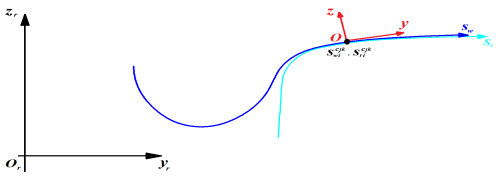

Figure 7: Normal abscissa for the wheel and rail profile.

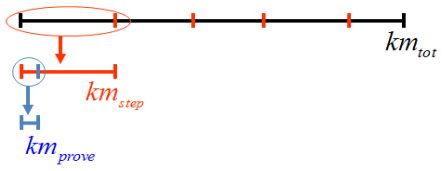

Figure 8: Discretization of the total mileage.

3. *Sum on the contact points*:

$$\Sigma_{i=1}^{N_{PDC}}\Delta_{P_{wi}^{jk}}(s_w)=\Delta_{jk}^{w}(s_w),\qquad \Sigma_{i=1}^{N_{PDC}}\Delta_{P_{ri}^{jk}}(s_r)=\Delta_{jk}^{r}(s_r) \tag{10}$$

where N_{PDC} is the maximum number of contact points of each single wheel (and respectively of each single rail).

4. *Evaluation of wheelset wear and class wear*:
introducing a new index to indicate the h-th vehicle wheelset, the average on the right and left wheels for each wheelset (commonly listed with odd and even index respectively) is carried out in order to consider the two-way traffic typical in railway vehicles:

$$\Delta^w_{hk}(s_w) = 1/2 \left(\Delta^w_{(2h)k}(s_w) + \Delta^w_{(2h-1)k}(s_w)\right)\Big|_{h=1}^{N_w/2}. \tag{11}$$

where N_w is the number of vehicle wheels. Then the following averages to evaluate for each wheelset the mean wear on all the N_c tracks and for each of the N_c class the mean rail wear considering all the wheel-rail pairs have been performed:

$$\Sigma_{k=1}^{N_c} p_k \Delta^w_{hk}(s_w) = \overline{\Delta}^w_h(s_w), \qquad \tfrac{1}{N_w}\Sigma_{j=1}^{N_w} \Delta^r_{jk}(s_r) = \overline{\Delta}^r_k(s_r). \tag{12}$$

5. *Scaling*:
the aim of the scaling procedure is to amplify the small quantity of material removed during the N_c dynamic simulations and, at the same time, to limit the computational load. Assuming the almost linearity of the wear model within a single step of the discrete procedure (a working hypothesis coming from the discrete approach of the model), it is possible to amplify the removed material by means of a suitable scaling factor based on the idea that the wear rate characterizing the performed simulations associated to the considered discrete step remains the same also inside the entire discrete step, since the vehicle always covers the same tracks both during the performed simulations and during the whole discrete step. In this work adaptive discrete steps (function of the wear rate) obtained imposing the threshold values D^w_{step} and D^r_{step} on the maximum of the material quantity to remove at each discrete step on the wheelsets and on the classes of curves respectively have been chosen to update the wheel and rail profiles (see eq. 13-18 and Fig. 8): in fact this method well fits in following the behavior of the wear evolution that could present non linear characteristics outside of the discrete steps. The evaluation of the discrete steps, with the consequent scaling of $\overline{\Delta}^w_h(s_w)$, $\overline{\Delta}^r_k(s_r)$ and $\Delta^{wSIM}_h(s_w)$, $\Delta^{rSIM}_k(s_r)$, represents the major difference between the update strategy of wheel and rail:

(a) the removed material on the wheel due to wear is proportional to the distance traveled by the vehicle; in fact a point of the wheel is frequently in contact with the rail in a number of times proportional to the distance. The following nomenclature can been introduced (see Figure 8): km_{tot} is the total mileage traveled by the considered vehicle, km_{step} is the length of the discrete step corresponding to the threshold value on the wear depth D^w_{step} and $km_{prove} = l_k$ is the overall mileage traveled by the vehicle during the N_c dynamic simulations. The necessity of acceptable computational time for the multibody simulations leads to adopt small values of the km_{prove} length and for this reason the relative removed material has to be scaled with a multiplicative factor. Finally the material removed on the wheels has to be scaled according to the following laws:

$$\overline{\Delta}^w_h(s_w)\tfrac{D^w_{step}}{D^w} = \overline{\Delta}^{wsc}_h(s_w), \qquad \overline{\Delta}^{wSIM}_h(s_w)\tfrac{D^w_{step}}{D^{wSIM}} = \overline{\Delta}^{wscSIM}_h(s_w) \tag{13}$$

$$km_{step} = \tfrac{D^w_{step}}{D^w} km_{prove}, \qquad km_{step}{}^{SIM} = \tfrac{D^w_{step}}{D^{wSIM}} km_{prove} \tag{14}$$

$$D^w = \max_h \max_{s_w} \overline{\Delta}^w_h(s_w), \qquad D^{wSIM} = \max_h \max_{s_w} \overline{\Delta}^{wSIM}_h(s_w). \tag{15}$$

The choice of the wear depth treshold must be a good compromise between numerical efficiency and the accuracy required by the wear model.

(b) the depth of rail wear is not proportional to the distance traveled by the vehicle; in fact the rail tends to wear out only in the zone where it is crossed by the vehicle and, increasing the traveled distance, the depth of removed material remains the same. On the other hand the rail wear is proportional to the total tonnage burden on the rail and thus to the total vehicle number N_{tot} moving on the track. Therefore, if N_{step} is the vehicle number moving in a discrete step, the quantity of rail removed material at each step will be:

$$\overline{\Delta}_k^r(s_r)\frac{D^r_{step}}{D^r} = \overline{\Delta}_k^{r\,sc}(s_r), \qquad \overline{\Delta}_k^{r\,SIM}(s_r)\frac{D^r_{step}}{D^{r\,SIM}} = \overline{\Delta}_k^{r\,scSIM}(s_r) \tag{16}$$

$$N_{step} = \frac{D^r_{step}}{D^r}N_{prove} \qquad , \qquad N_{step}{}^{SIM} = \frac{D^r_{step}}{D^{r\,SIM}}N_{prove}, \qquad N_{prove} = 1 \tag{17}$$

$$D^r = \max_k \max_{s_r} \overline{\Delta}_k^r(s_r), \qquad D^{r\,SIM} = \max_k \max_{s_r} \overline{\Delta}_k^{r\,SIM}(s_r). \tag{18}$$

6. *Smoothing of the removed material*:

$$\Im\left[\overline{\Delta}_h^{wsc}(s_w)\right] = \overline{\Delta}_{h\,sm}^{wsc}(s_w), \quad \Im\left[\overline{\Delta}_k^{r\,sc}(s_r)\right] = \overline{\Delta}_{ksm}^{r\,sc}(s_r); \tag{19}$$

the smoothing of the removed material function is necessary to remove the numerical noise that affects this quantity and that would be passed to the new profiles $\tilde{w}_n(s_w)$, $\tilde{r}_n(s_r)$ and $\tilde{w}_n^{SIM}(s_w)$, $\tilde{r}_n^{SIM}(s_r)$ of wheel and rail causing problems to the global contact models. To this end, a discrete filter (i. e. a moving average filter with window size equal to $1\% \div 5\%$ of the total number of points in which the profiles are discretized) has been used; obviously the discrete filter has to conserve the mass.

7. *Profile update:*

$$\begin{pmatrix} y_w(s_w) \\ \tilde{w}_o(s_w) \end{pmatrix} - \overline{\Delta}_{h\,sm}^{wsc}(s_w)\mathbf{n}_w^r \xrightarrow{re-parameterization} \begin{pmatrix} y_w(s_w) \\ \tilde{w}_n(s_w) \end{pmatrix}, \begin{pmatrix} y_r(s_r) \\ \tilde{r}_o(s_r) \end{pmatrix} - \overline{\Delta}_{ksm}^{r\,sc}(s_r)\mathbf{n}_r^r \xrightarrow{re-parameterization} \begin{pmatrix} y_r(s_r) \\ \tilde{r}_n(s_r) \end{pmatrix} \tag{20}$$

the last step consists in the update of the old profiles $\tilde{w}_o(s_w) = w_o(y_w)$, $\tilde{w}_o^{SIM}(s_w) = w_o{}^{SIM}(y_w)$ and $\tilde{r}_o(s_r) = r_o(y_r)$, $\tilde{r}_o^{SIM}(s_r) = r_o{}^{SIM}(y_r)$ to obtain the new profiles $\tilde{w}_n(s_w) = w_n(y_w)$, $\tilde{w}_n^{SIM}(s_w) = w_n{}^{SIM}(y_w)$ and $\tilde{r}_n(s_r) = r_n(y_r)$, $\tilde{r}_n^{SIM}(s_r) = r_n{}^{SIM}(y_r)$; since the removal of material occurs in the normal direction to the profiles ($\mathbf{n_w^r}$ and $\mathbf{n_r^r}$ are the outgoing unit vectors for the wheel and rail profiles respectively), once removed the quantities $\overline{\Delta}_{h\,sm}^{wsc}(s_w)$, $\overline{\Delta}_{h\,sm}^{wsc\;SIM}(s_w)$ and $\overline{\Delta}_{ksm}^{r\,sc}(s_r)$, $\overline{\Delta}_{ksm}^{r\,sc\;SIM}(s_r)$, a re-parameterization of the profiles is needed in order to obtain again curves parameterized by means of the curvilinear abscissa.

5 WEAR MODEL VALIDATION

In this section the comparison between the developed wear model and the SIMPACK one will be presented. Initially the procedure used to extract the statistical description of the Italian railway net will be introduced. Then the wear control parameters for the wheel and rail will be showed. Finally, the simulation strategy used to analyze the wear both on the wheel and on the rail will be described and the results obtained with the UNIFI wear model will be analyzed and compared with the SIMPACK wear model.

5.1 The statistical approach

The statistical approach to the track has been chosen to reduce and rationalize the total simulation work, avoiding excessively long simulations on the real track. The idea is to substitute the simulation on the whole track (the Italian railway net) with a statistically equivalent set of N_c simulations on short curved tracks.

Starting from the data of the whole Italian railway net (provided by RFI), the statistical analysis has been performed by dividing the line in radius classes (determined by R_m and R_M) and each of these in superelevation classes (determined by an h_{range}) [4]. The subclasses that do not include curve have not been taken into account in the definition of the set of N_c tracks; all the N_c curved tracks are shown in Table 1.

The set consists in $N_c = 33$ distinct elements (32 real curves and the straight line) characterized by a mean radius value R_r, the superelevation value h_r, the traveling speed V_r and the statistical weight p_k (with $1 \leq k \leq N_c$) that represents the frequency with which each curve appears on the considered railway track. The radii R_r are calculated by means of the weighted mean on all the curve radii included in the corresponding superelevation subclass (the weighted factor is the length of the curves in the real track). For each subclass, the value h_r is the most frequent superelevation value among the standard values that characterize the curves of the considered superelevation subclass. The traveling speeds V_r are calculated imposing a threshold value on the uncompensated acceleration $a_{nc}^{lim} = 0.6m/s^2$, $\frac{\tilde{V}^2}{R_c} - \frac{H}{s}g = a_{nc}^{lim}$ where s is the railway gauge and g is the gravity acceleration. The estimated speed $\tilde{V}$ has been then compared with the maximum velocity V_{max} on the line to get the desidered traveling speed $V_r = min\left(\tilde{V}, V_{max}\right)$.

Table 1: Virtual track.

R_m (m)	R_M (m)	R_r (m)	h_{range} (mm)	h_r (mm)	V_r (km/h)	p_k %
278	313	**294**	90–120	100	70	0.04
			130–160	140	75	0.03
313	357	**333**	90–120	120	75	0.74
			130–160	160	85	0.74
357	417	**385**	50–80	60	70	0.82
			90–120	90	70	0.07
			130–160	160	85	0.19
417	500	**455**	50–80	50	70	0.03
			90–120	120	90	0.20
			130–160	150	100	1.76
500	625	**556**	10–40	30	70	0.02
			50–80	60	70	0.15
			90–120	120	95	0.36
			130–160	140	105	1.29
625	833	**714**	10–40	20	70	0.03
			50–80	80	90	0.25
			90–120	90	95	1.14
			130–160	160	130	1.93
833	1250	**1000**	10–40	40	70	0.07
			50–80	80	105	1.87
			90–120	120	130	1.80
			130–160	160	150	2.05
1250	2500	**1667**	0	0	70	0.09
			10–40	40	95	0.56
			50–80	80	140	2.27
			90–120	110	160	1.78
			130–160	160	160	0.73
2500	10000	**5000**	0	0	70	0.51
			10–40	30	145	3.96
			50–80	50	160	2.12
			90–120	90	160	0.003
		∞			160	74.4

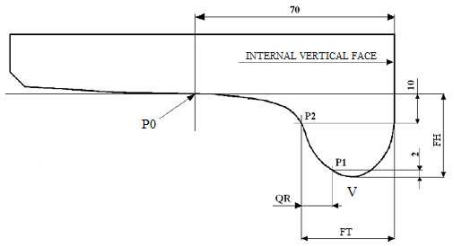

(a) Definition of the wheel control parameters.

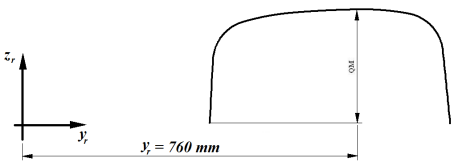

(b) Definition of rail control parameter.

Figure 9: Wear reference dimensions.

5.2 Wear Control Parameters

The reference quotas FH, FT and QR are introduced in order to estimate the wheel profile evolution due to the wear without necessarily knowing a complete detection of the profile shape (see Figure 9(a)). According to these quotas it will be possible both to establish when the worn wheel profile will have to be re-profiled and to detect if the wear compromises the dynamical

stability of the vehicle [2].

In regard to their physical meaning, both the flange thickness FT and the flange height FH describe the size of the flange, while the flange height is also a measure of the wear on the wheel tread. The QR dimension gives information related to the conicity of the flange.

An additional control parameter is then introduced to evaluate the evolution of rail wear. Particularly the QM quota is defined as the rail head height in the point $y_r = 760\ mm$ with respect to the center line of the track: this y_r value depends on the railway gauge (equal to 1435 *mm* in the Italian railway line) and on the laying angle α_p of the track (equal to 1/20 rad). Physically the QM quota gives information on the rail head wear (see Figure 9(b)).

5.3 Simulation Strategy

In this section the simulation campaign performed to study the wear on wheel and rail is described. As explained in section 4.4, the two phenomena evolve according to different time scales (several orders of magnitude) and a fully simulation of such events would require a too heavy computational effort. For this reason the following specific algorithm has been adopted for updating the profiles:

1. a suitable number of discrete steps both for the wheel and for the rail has been chosen, $n_{sw} = 15$ and $n_{sr} = 5$, so to have a good compromise between calculation times and result accuracy. Consequently the wheel wear threshold D^w_{step} (see section 4.4) has been chosen equal to 0.4 *mm* and the value of the rail wear threshold D^r_{step} (see section 4.4) has been set equal to 0.8 *mm* to obtain an appreciable rail wear during the simulations.

2. the wear evolution on wheel and rail has been decoupled because of the different scales of magnitude. While the wheel wear evolves, the rail is supposed to be constant: in fact, in the time scale considered, the rail wear variation is negligible. On the other hand, because of the time scale characteristic of the rail wear, each discrete rail profile comes in contact, with the same frequency, with each possible wheel profile; for this reason, for each rail profile, the whole wheel wear evolution (from the original profile to the final profile) has been simulated.

Based on the two previous hypotheses, the simulations have been carried out according to the following strategy:

$$
\begin{array}{l}
\textbf{Wheel profile evolution at first rail step: } w_{h_i}^{\ 0} \\
p_{1,1}\left\{\begin{pmatrix} w_{h0}^{0} & r_{k0} \end{pmatrix} \rightarrow \begin{pmatrix} w_{h1}^{0} & r_{k0} \end{pmatrix} \rightarrow \ldots \rightarrow \begin{pmatrix} w_{hn_{sw}-1}^{0} & r_{k0} \end{pmatrix} \rightarrow w_{hn_{sw}}^{0}\right. \\
\\
\textbf{Average on the rails } r_{k1}^{(i+1)} \textbf{ for the calculation of the second rail step: } r_{k1} \\
p_{1,2}\left\{\begin{pmatrix} w_{h0}^{0} & r_{k0} \\ w_{h1}^{0} & r_{k0} \\ \vdots & \vdots \\ w_{hn_{sw}-1}^{0} & r_{k0} \end{pmatrix} \rightarrow \begin{pmatrix} r_{k1}^{(1)} \\ r_{k1}^{(2)} \\ \vdots \\ r_{k1}^{(n_{sw})} \end{pmatrix} \rightarrow r_{k1}\right. \\
\vdots \\
\\
\textbf{Wheel profile evolution at fourth rail step: } w_{h_i}^{n_{sr}-1} \\
p_{n_{sr},1}\left\{\begin{pmatrix} w_{h0}^{n_{sr}-1} & r_{kn_{sr}-1} \end{pmatrix} \rightarrow \begin{pmatrix} w_{h1}^{n_{sr}-1} & r_{kn_{sr}-1} \end{pmatrix} \rightarrow \ldots \rightarrow \begin{pmatrix} w_{hn_{sw}-1}^{n_{sr}-1} & r_{kn_{sr}-1} \end{pmatrix} \rightarrow w_{hn_{sw}}^{n_{sr}-1}\right. \\
\\
\textbf{Average on the rails } r_{kn_{sr}}^{(i+1)} \textbf{ for the calculation of the fifth rail step: } r_{kn_{sr}} \\
p_{n_{sr},2}\left\{\begin{pmatrix} w_{h0}^{n_{sr}-1} & r_{kn_{sr}-1} \\ w_{h1}^{n_{sr}-1} & r_{kn_{sr}-1} \\ \vdots & \vdots \\ w_{hn_{sw}-1}^{n_{sr}-1} & r_{kn_{sr}-1} \end{pmatrix} \rightarrow \begin{pmatrix} r_{kn_{sr}}^{(1)} \\ r_{kn_{sr}}^{(2)} \\ \vdots \\ r_{kn_{sr}}^{(n_{sw})} \end{pmatrix} \rightarrow r_{kn_{sr}}\right.
\end{array}
\tag{21}
$$

where $w_{h_i}^{\ j}$ indicates, for the h-th wheelset, the i-th step of the wheel profile that evolves on j-th step of the k-th rail profile r_{kj} with $0 \le i \le n_{sw}-1$, $0 \le j \le n_{sr}-1$, $1 \le k \le N_c$ and $1 \le h \le N_w/2$. The initial profiles $w_{h0}^{\ j}$ are always the same for each j and correspond to the unworn wheel profile.

Initially the wheel (starting from the unworn profile w_{h0}^0) evolves on the unworn rail profile r_{k0} in order to produce the discrete wheel profiles $w_{h0}^0, w_{h1}^0, ..., w_{hn_{sw}}^0$ (step $p_{1,1}$). Then the virtual rail profiles $r_{k1}^{(i+1)}$, obtained by means of the simulations (w_{hi}^0, r_{k0}) with $0 \leq i \leq n_{sw} - 1$, are arithmetically averaged so as to get the update rail profile r_{k1} (step $p_{1,2}$). This procedure can be repeated n_{sr} times in order to perform all the rail discrete steps (up to the step $p_{n_{sr},2}$). The characteristics of the processor used in the simulations and the mean computational times relative to each discrete step of the whole model loop are schematically summarized in Tab. 2. The main numerical parameters relative to the integrator used for the dynamical simulations of both the models are briefly reported in Tab. 3. The UNIFI model, thanks to the high numerical

Table 2: Computational time.

Wear Model	Processor	Computational time	
		Dynamic simulation	Wear simulation
UNIFI	INTEL Xeon CPU E 5430 2.66 GHz 8GB RAM	38min	9min
SIMPACK		1h 2min	4min

Table 3: Integrator parameters.

Integrator type	ODE5
Alghoritm	DoPri
Order	5
Step type	fixed
Stepsize	10^{-4} s

efficiency of the new global contact model (see section 3.2.1) is rather faster than the SIMPACK one despite the latter uses approximated look-up tables for evaluating the global contact parameters. On the other hand the heavy approximation of the global wear evaluation approach of the SIMPACK model leads to a lower wear simulation time than that of the UNIFI model where the contact patch investigation obviously has an impact on the computational load.

5.4 Evolution of Wear Control Parameter

In this section the evolution both of the wheel reference quotas (flange thickness FT, flange height FH and flange steepness QR) and of the rail reference quota QM numerically evaluated by means of the developed wear model will be compared with the SIMPACK model results. The wheel quotas are shown as a function of the n_{sw} wheel steps while the QM parameter is shown as a function of the rail steps n_{sr}. For reasons of brevity only the wheel quotas related to the first and the last rail steps (r_{k0} and r_{k4}) will be shown together with the rail quota QM. For the same reasons only the results related to the head vehicle (E.464 locomotive) will be presented considering that the first vehicle is the most critical from a wear viewpoint because of the vehicle dynamics.

In Fig. 10, 13 the comparison between the FT dimensions for the two wheelsets of the front bogie of the E.464 locomotive coach is presented. As it can be seen the thickness of the leading wheel (w_{1i}, ${w_{1i}}^{SIM}$) decreases more than the same quantity of the rear wheel (w_{2i}, ${w_{2i}}^{SIM}$). It is due to the vehicle dynamics (different load distribution on the wheels) and to the particular position of the wheelset inside the bogie; the rear wheel of each bogie has a smoothing curve entry because of the guide effects of the bogie itself.

The FH quota progresses are represented in Fig. 11, 14 and show that the wheel wear on the tread is appreciable mainly for the first rail step (i.e. UIC60 unworn rail profile), due to the more conformal contact between the wheel and rail surfaces as the rail wear increases. Also the FH dimension displays more wear on the leading wheel while for the rear wheel the tread wear is lower in all studied cases.

The QR trend are shown in Fig. 12, 15; the flange steepness decreases leading to an increase of the conicity of the flange; also for this dimension the considerations related to the leading

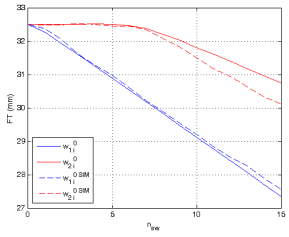

Figure 10: E.464: FT progress at r_{k0} rail step.

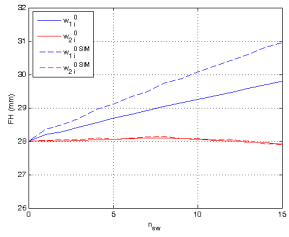

Figure 11: E.464: FH progress at r_{k0} rail step.

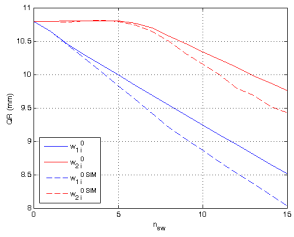

Figure 12: E.464: QR progress at r_{k0} rail step.

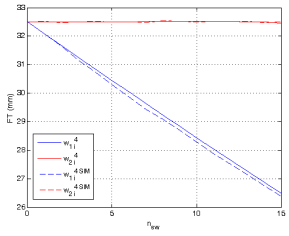

Figure 13: E.464: FT progress at r_{k4} rail step.

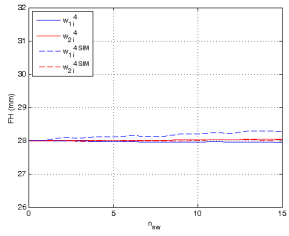

Figure 14: E.464: FH progress at r_{k4} rail step.

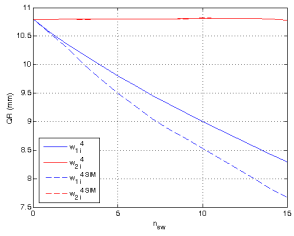

Figure 15: E.464: QR progress at r_{k4} rail step.

and rear wheel hold. Regards to the wheel reference dimensions all the proposed considerations hold also for the Vivalto coach.

In Fig. 16 the QM evolution for the wear rail can be seen: for the sake of clarity the wear progress of only three of the N_c curves are represented (the first, the sixteenth and the thirty-first curves). The QM trend shows that the rail wear increases with the curve radius decreases according with the real wear phenomena (see Tab. 1: r_{1j} is referred to the minimum curve radius, r_{16j} to an intermediate one while r_{31j} to the maximum curve radius).

In conclusion the comparison of the reference dimensions leads to a good qualitative agreement between the developed wear model and the SIMPACK one; both the models show the same wear behavior concerning leading and rear wheelsets, contact conformity and curve radius.

In Fig. 17 the evolution of the km_{step} as a function of the wheel discrete step number n_{sw} is shown (for brevity only the km_{step} related to the first and the latter rail step are presented). Related to the first rail step r_{k0} the lower km_{step} values and their higher gradient in the first wheel steps indicate the higher wear rate due to the initial non conformal contact characterizing the coupling between the new wheel profile ORE S1002 and rail profile UIC60 with laying angle equal to 1/20; the almost constant values in the latter steps (combined with higher km_{step} values) show at the same time the achievement of a more and more conformal contact as the wheel wear increases. Considering the latter rail step r_{k4} the same curve trend can be seen but characterized by higher km_{step} values because of the worn rail profile that leads to an initial more conformal contact than the previous case. In Fig. 18 the evolution of the N_{step} as a function of the rail discrete number n_{sr} is shown and it can be seen that the considerations referred to the variation of the contact conditions (conformity) hold also in this case.

The Tables 4, 5 show the overall mileages km_{tot}^{j} traveled by the vehicle composition for each rail step r_{kj} and the total vehicle number N_{tot} burden on the track during the overall wear loop. The increase of the total mileage as the rail profile is more and more worn is caused by the increase of the conformity between wheel and rail surfaces. Finally, analyzing the difference between the UNIFI and the SIMPACK model the Fig. 17 and the Tab. 4 show, on average,

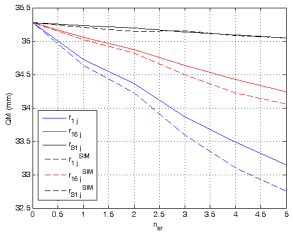

Figure 16: QM progress.

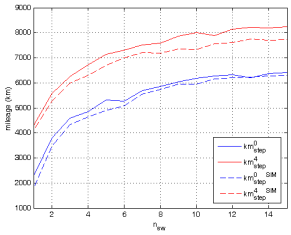

Figure 17: km_{step} evolution.

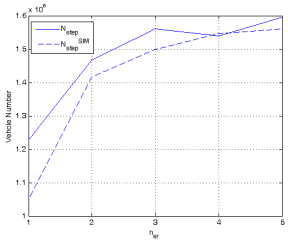

Figure 18: N_{step} evolution.

Table 4: Evolution of the km_{tot}.

Wear Model	km^0_{tot} (km)	km^1_{tot} (km)	km^2_{tot} (km)	km^3_{tot} (km)	km^4_{tot} (km)
UNIFI	81460	88120	94350	102080	108950
SIMPACK	78530	84870	92020	98210	102790

Table 5: Evolution of the N_{tot}.

Wear Model	N_{tot}
UNIFI	7390900
SIMPACK	7074500

lower km_{step} values in the SIMPACK case that indicate an increase of the wheel wear due to the probably wear overestimation caused by the global wear approach of the SIMPACK model that, not considering the subdivision of the contact patch in slip and adhesion zone, lead to substract the removed material due to wear in overall the contact patch itself; the same observation hold for the vehicle number N_{step} as can be seen in Fig. 18 and Tab. 5.

5.5 Evolution of the Wheel and Rail Profile

The wear evolution on the wheel profiles evolving on the first and on the latter rail step r_{k0}, r_{k4} for the wheelsets of the front bogie of the E.464 vehicle is presented in the Fig. 19-26. As stated previously, the wheel profile evolution is described by means of $n_{sw} = 15$ steps and the threshold on the removed material for each step D^w_{step} has been chosen equal to 0.4 *mm*. From the figures it can be seen both the wear increase on the leading wheel with respect to the rear wheel of the bogie and the wheel wear decrease when the wheel is coupled with the worn rail profile r_{k4} with respect to the unworn profile r_{k0} due to the achievement of the conformal contact in the wheel-rail pairs.

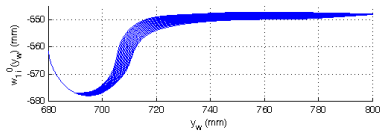

Figure 19: UNIFI model: E.464 $w_{1_i}^0$ evolution.

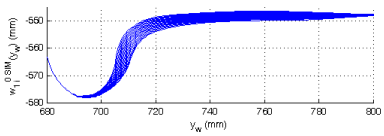

Figure 20: SIMPACK model: E.464 $w_{1_i}^0$ evolution.

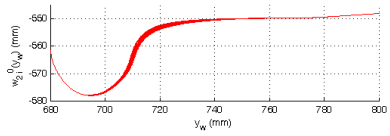

Figure 21: UNIFI model: E.464 $w_{2_i}^0$ evolution.

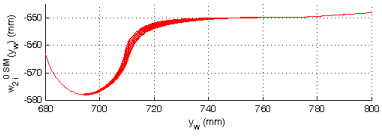

Figure 22: SIMPACK model: E.464 $w_{2_i}^0$ evolution.

In Fig. 27-32 the rail profile evolutions related to the three different curves of the statistical analysis r_{1j}, r_{16j} and r_{31j} are presented; the removed material due to wear shows a rather clear dependence from the curve radius and in particular the wear increases in the sharp curves

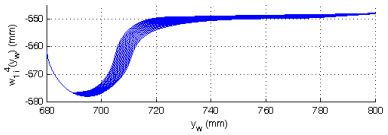

Figure 23: UNIFI model: E.464 $w_{1_i}^4$ evolution.

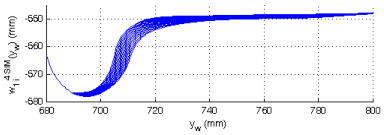

Figure 24: SIMPACK model: E.464 $w_{1_i}^4$ evolution.

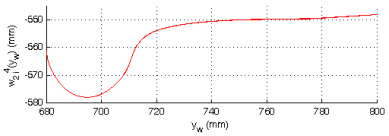

Figure 25: UNIFI model: E.464 $w_{2_i}^4$ evolution.

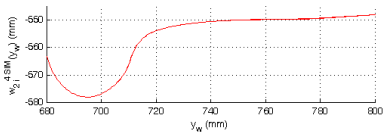

Figure 26: SIMPACK model: E.464 $w_{2_i}^4$ evolution.

because of the resulting vehicle dynamics and harder contact conditions. In all the studied cases the comparison between the profile evolutions obtained with the innovative developed wear model and the SIMPACK one results rather satisfactory without pronounced differences.

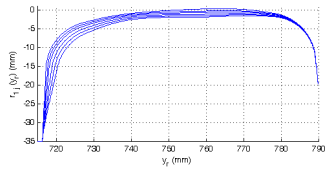

Figure 27: UNIFI: $r_{1\,j}$ evolution.

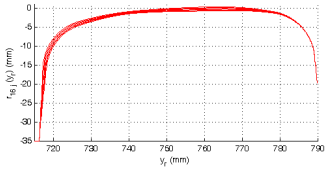

Figure 28: UNIFI: $r_{16\,j}$ evolution.

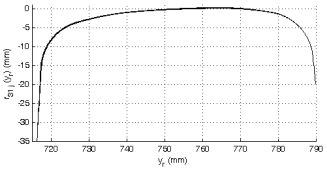

Figure 29: UNIFI: $r_{31\,j}$ evolution.

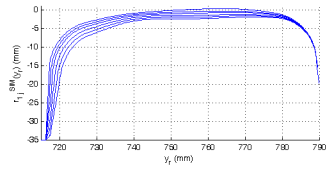

Figure 30: SIMPACK: $r_{1\,j}{}^{SIM}$ evolution.

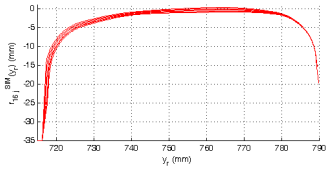

Figure 31: SIMPACK: $r_{16\,j}{}^{SIM}$ evolution.

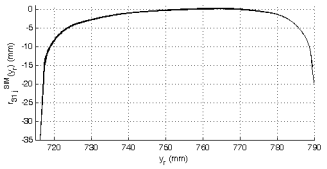

Figure 32: SIMPACK: $r_{31\,j}{}^{SIM}$ evolution.

6 CONCLUSIONS

In this work Authors presented a complete model for the wheel and rail wear prediction in railway application, developed thanks to the collaboration with Trenitalia S.p.A and Rete Ferroviaria Italiana (RFI), which provided the necessary technical data referred to a vehicle composition widely used in Italian railways (E.464 locomotive and Vivalto coach) and the track data related to the whole Italian railway net. The whole model is made up of two mutually interactive parts; the *vehicle model* made up of the multibody model and the global contact model and the *wear model* consisting in local contact model, wear evaluation procedure and profile updating. The performance of the innovative model have been compared with the wear evaluation procedure implemented within the Simpack multibody commercial software in order to have a further validation of the model besides the wheel wear validation referred to the quite short critical scenario of the Aosta-Pre Saint Didier line performed in previous works [4]. The comparison has been carried out, from the track viewpoint, on the whole Italian railway

net, analyzed by means of a statistical approach to reduce the total computational load; the vehicledynamics and the wear evolution have been then simulated on the N_c curvilinear tracks of the statistical analysis. The results obtained in this research highlight how the innovative model reflects the typical behavior of the wear phenomena (for example an higher removed material for the leading wheel and for the sharp curves and a wear decrease when the contact conditions achieve the conformal contact). On the other hand the comparison with the Simpack wear model has given satisfactory results both in terms of reference dimensions and profiles evolution; the only evident difference is a little wear overestimation of the SIMPACK model probably due to the approximated global wear approach that does not consider the division of the contact patch in adhesion and slip zone.

Future developments will be based on further experimental data (relative to other railway track with an higher mileage than the Aosta-Pre Saint Didier line used in previous works) provided by Trenitalia and RFI and referred to advanced wear on the wheel (especially on the wheel tread) and on the rail. In this way other analysis will be carried out in order to further validate the whole model. Moreover the design of new wheel and rail profiles as well as of new bogie shapes and suspension stages optimized from the wear viewpoint will be performed according to the research interests of Trenitalia.

ACKNOWLEDGEMENTS

Authors would like to thank Engg. R. Cheli and G. Grande of Trenitalia S.p.A. for providing and giving the permission to edit the data relative to the vehicle composed by the E.464 locomotive and the Vivalto passenger coach; a special thanks also goes to the Engg. R. Mele and M. Finocchi of Rete Ferroviaria Italiana for the data relative to the whole Italian railway net.

REFERENCES

[1] Multi-body simulation simpack mbs software: http://www.simpack.com/.

[2] EN 15313: Railway applications — In-service wheelset operation requirements — In-service and off-vehicle wheelset maintenance, 2010.

[3] J. Auciello, E. Meli, S. Falomi, and M. Malvezzi. Dynamic simulation of railway vehicles: wheel/rail contact analysis. *Vehicle System Dynamics*, 47:867–899, 2009.

[4] M. Ignesti, M. Malvezzi, L. Marini, E. Meli, and A. Rindi. Development of a wear model for the prediction of wheel and rail profile evolution in railway systems. *Wear*, 2012. DOI: 10.1016/j.wear.2012.01.020.

[5] S. Iwnicki. *The Manchester Benchmarks for Rail Vehicle Simulators*. Swets and Zeitlinger, Lisse, Netherland, 1999.

[6] J. J. Kalker. *Three-dimensional Elastic Bodies in Rolling Contact*. Kluwer Academic Publishers, Dordrecht, Netherlands, 1990.

[7] H. Krause and G. Poll. Verschleibei gleitender und wlzender relativbewegung. *Tribologie und Schmierungstechnik*, 31:issue 4/5, 209–214/285–289, 1984.

[8] A. A. Shabana, M. Tobaa, H. Sugiyama, and K. E. Zaazaa. On the computer formulations of the wheel/rail contact problem. *Nonlinear Dynamics*, 40:169–193, 2005.